IOPscience iopscience.iop.org

Home Search Collections Journals About Contact us My IOPscience

Positron lifetime in oxide superconductors $YBa_2(Cu_{1-x}M_x)O_{7-y}$ (M=Fe, Ni, Zn)

This article has been downloaded from IOPscience. Please scroll down to see the full text article.

1991 J. Phys.: Condens. Matter 3 9169

(http://iopscience.iop.org/0953-8984/3/46/018)

View the table of contents for this issue, or go to the journal homepage for more

Download details:
IP Address: 171.66.16.96
The article was downloaded on 10/05/2010 at 23:50

Please note that terms and conditions apply.

J. Phys.: Condens. Matter 3 (1991) 9169–9184. Printed in the UK

Positron lifetime in oxide superconductors $YBa_2(Cu_{1-x}M_x)_3O_{7-y}$ (M = Fe, Ni, Zn)

Shoji Ishibashi†‖, Ryoichi Yamamoto†, Masao Doyama‡ and Takehiko Matsumoto§

† Research Center for Advanced Science and Technology, The University of Tokyo, 4-6-1 Komaba, Meguro-ku, Tokyo 153, Japan

‡ Department of Materials Engineering, The Nishi Tokyo University, Uenohara, Kitatsuru-gun, Yamanashi 409-01, Japan

§ National Research Institute for Metals, 2-3-12 Nakameguro, Meguro-ku, Tokyo 153, Japan

Received 11 June 1991

Abstract. We present the temperature dependence of positron lifetime parameters measured on a series of specimens of $YBa_2(Cu_{1-x}M_x)_3O_{7-y}$ (M = Fe, Ni, Zn) in the temperature range 20–300 K. In a non-doped specimen, the defect-related component τ_2 showed a step-like increase in the temperature range 40–100 K. Above 180 K, the mean lifetime τ_{mean} decreased with increasing temperature. These variations in τ_2 or τ_{mean} are explained in terms of a thermally activated escape of positrons from the two kinds of trapping centres. The bulk lifetime τ_{bulk} showed a slight decrease in the region 100–300 K. The iron doping moved the shift of the transition region of τ_2 towards a higher temperature and removed the decrease of τ_{mean} out of the temperature range in which experiments were performed. These phenomena are ascribed to the enhancement of the positron–defect binding energies, which is theoretically predicted. On the other hand, nickel and zinc did not much alter the behaviour of τ_2, but affected that of τ_{bulk}. A direct correlation between the superconducting critical temperature (Tc) and the lifetime–temperature curve was not found.

1. Introduction

Novel oxide superconductors [1–5], which have been found since the discovery of superconductivity in the La–Ba–Cu–O system by Bednorz and Müller [1], have been attracting a huge amount of attention because they not only have rather high superconducting critical temperatures but also various anomalous properties. A lot of experimental techniques have been applied in the study of the anomalies of these materials as well as in high-T_c superconductivity.

Positron annihilation experiments, which are useful in the study of electronic or defect structures of condensed matter [6], have been also performed from two points of view. One is the temperature variation of positron annihilation parameters, such as the S parameter of the Doppler broadened spectra of annihilation quanta and positron lifetime. The other is the momentum distribution of annihilation quanta. The latter is directly correlated with the problem of whether or not a Fermi surface exists in oxide

‖ Present address: Electrotechnical Laboratory, 1-1-4 Umezono, Tsukuba, Ibaraki 305, Japan.

0953-8984/91/469169 + 16 $03.50 © 1991 IOP Publishing Ltd

superconductors, and has generated much interest. However, conclusive results have not been obtained [7]. As for the former, the first experiment was performed by the present authors [8]. Anomalous thermal behaviour of the S parameter in the La–Sr–Cu–O and Y–Ba–Cu–O systems was observed. Subsequently, a number of measurements of the S parameter and/or lifetime have been performed, mainly on YBCO [9].

The results obtained are largely scattered although some common features exist among them. The discrepancy in the results is in part due to incompleteness of the sample characterizations at the early stages of these studies, as in other experiments. The predominant reason for the discrepancy is the variation of lattice defects existing in the samples. Each type of defect corresponds to a distinct value of the S parameter or a positron lifetime. The amount of each defect is reflected in the contribution of the positron annihilation at the defect to the total events.

The reproducible and common features among the results of the S parameter, or mean lifetime, can be classified into two categories: (i) a positive temperature dependence below ~100 K [8, 10–19] and (ii) a negative temperature dependence above ~100 K [16, 18, 20, 21]. A step-like increase around ~80 K sometimes coexists with the first-type temperature dependence [10, 16, 19]. Since the temperature variation of a defect-related lifetime component belongs to the first-type [10, 11, 21–23], the first-type temperature dependence can be ascribed to the positron annihilation at defects, while the second type can be ascribed to the annihilation in the bulk of the specimen. A few different types of temperature dependence of the annihilation parameters are also reported. Harshmann *et al* have performed the measurements on a single-crystal of YBCO and obtained a single lifetime component which shows negative temperature dependence below ~80 K [24]. Teng *et al* [25], Zhu *et al* [26] and Krištiaková *et al* [27] reported resonant behaviour of the annihilation parameters at T_c.

The relationship between the superconductivity and the positron lifetime results has become a matter of concern. In order to examine the relationship, experimentation on a series of samples whose T_c varies systematically is of great use. The T_c can be controlled by substituting for copper with a metal impurity as well as by varying oxygen stoichiometry.

Recently, we performed preliminary experiments of positron lifetime measurements on iron or nickel doped YBCO and found a strong dependence of the lifetime, and its thermal behaviour, on the dopant content, especially in the iron case [28, 29]. A plausible explanation was given in terms of the shallow trapping of positrons.

In this paper, we present experimental results of measurements of positron lifetime in $YBa_2(Cu_{1-x}M_x)_3O_{7-y}$ (M = Fe, Ni, Zn) as well as theoretical estimations of distributions, lifetimes and energy eigenvalues of positrons therein. The purposes of the present work are (i) to establish a model explaining the temperature variation of the defect-related component, (ii) the same for the bulk component; and (iii) to clarify the relationship between the superconductivity and each component.

2. Calculations of positron distribution, lifetime and energy eigenvalues

Calculations were performed using the method developed by Puska and Nieminen [30]. The positron potential $V(r)$ is denoted as

$$V(r) = V_C(r) + V_{corr}(n_-(r)) \tag{1}$$

where V_C is a coulombic potential from nuclei and electrons while V_{corr} is a correlation

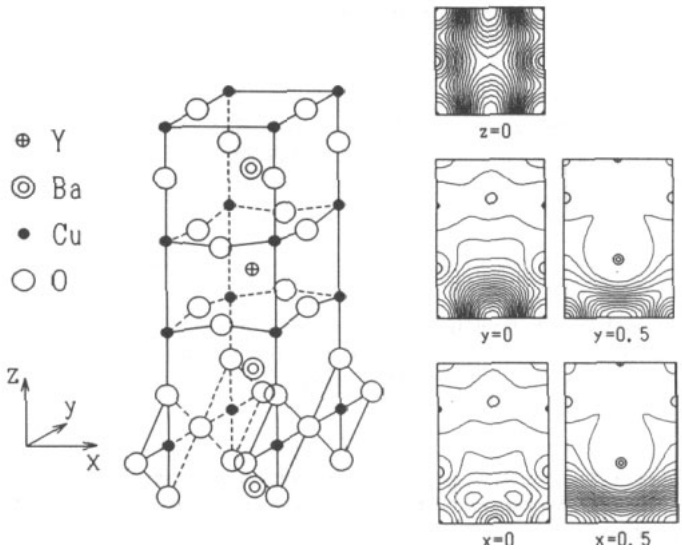

Figure 1. Crystal structure of YBCO and the positron distribution therein. A positron predominantly distributes between the CuO one-dimensional chains.

potential due to positron–electron correlation effects. The practical form of V_{corr} as a function of $n_-(r)$ was given by Boroński and Nieminen [31]. $n_-(r)$ and $V_C(r)$ were obtained by the superposition of atomic electron densities and potentials [32]. The positron Schrödinger equation can be solved by the numerical relaxation technique proposed by Kimball and Shortley [33]. The differential equation is replaced by a set of linear algebraic equations on a set of three-dimensional mesh points.

The positron lifetime is obtained as the inverse of the annihilation rate, which is represented as follows:

$$\lambda = \pi r_0^2 c \int \mathrm{d}r\, n_+(r)\left(n_v(r)\Gamma_v(n_v(r)) + n_c(r)\Gamma_c\right) \tag{2}$$

where r_0 is the classical electron radius, c is the speed of light, n_+, n_v and n_c represent densities of positron, valence electrons and core electrons respectively and Γ_v and Γ_c are the enhancement factors for valence and core electrons. We used the Brandt–Reinheimer expression [34] for the former and a constant value of 1.5 for the latter.

The mesh spacings were taken to be 0.05–0.1 times a_0, b_0 and $c_0/3$ (a_0, b_0, c_0: lattice parameters) along each direction. Practical calculations were performed on a one-eighth volume of the objective cells using crystal symmetry. The electrons in the orbitals of the Cu 3d and 4s, the O 2p, the Y 4d and 5s, and the Ba 6s have been taken as the valence electrons. We used the structural data obtained by Jorgensen *et al* [35].

The positron distribution obtained in the perfect crystal of YBCO is shown together with the crystal structure in figure 1. Here, a Cu(1) site is taken as the origin of the coordinates. Positrons predominantly distribute along the Cu–O one-dimensional chains. The corresponding positron lifetime is estimated to be 159 ps.

We have also calculated the distribution etc of positrons trapped at oxygen vacancy clusters. Figure 2 shows (*a*) the distribution of positrons trapped at an isolated oxygen

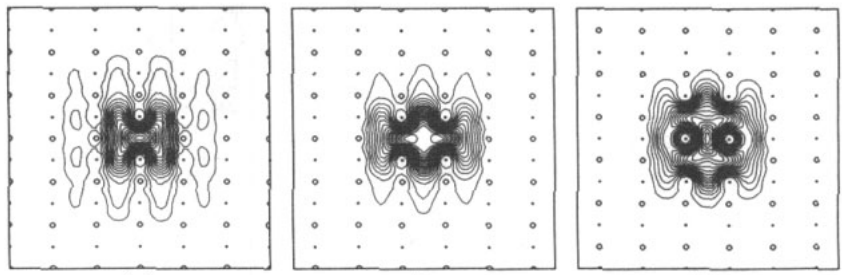

Figure 2. Distributions of positrons trapped at (*a*) an isolated oxygen vacancy, (*b*) a vacancy cluster containing two oxygen vacancies and (*c*) a vacancy cluster with four oxygen vacancies. A positron tends to localize with growing cluster size.

Table 1. The calculated positron lifetime and binding energy between the positron and the oxygen vacancy clusters. With growing cluster size, both the lifetime and the binding energy increase.

Cluster size	Positron lifetime	Binding energy
1	171 ps	73 meV
2	181 ps	114 meV
4	190 ps	266 meV

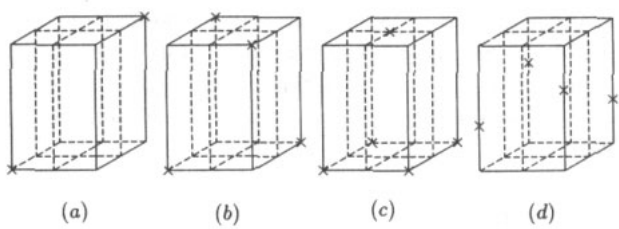

Figure 3. Structural models used for the calculation of positron distributions in impurity-doped YBCO; (*a*) Cu(1) site 2.1%, (*b*) Cu(1) site 4.2%, (*c*) Cu(1) site 8.3% and (*d*) Cu(2) site 8.3%. The positions of the impurity atoms are represented by crosses.

vacancy, (*b*) *a vacancy cluster containing two oxygen vacancies* and (*c*) the same but with four oxygen vacancies. The positron lifetimes and binding energies corresponding to the defects are shown in table 1. With the cluster size varying from 1 to 4, the positron state is more localized and the binding energy is enhanced. The lifetime value also increases from 171 ps to 189 ps.

Substitution effects are examined using the structural models shown in figure 3. These models are the one-eighth volumes of the objective unit cells, in which the positron wave-function is to be calculated. The models, figures 3(*a*), (*b*) and (*c*), correspond to the substitutions at the Cu(1) site with concentrations of 2.1%, 4.2% and 8.3% respectively, while the model, figure 3(*d*), represents the substitution at the Cu(2) with a concentration of 8.3%. It has been revealed by neutron diffraction measurements

[36–39] and EXAFS experiments [40] that most iron atoms occupy the Cu(1) site. As for nickel or zinc substitution, conflicting conclusions were drawn by several groups. Kajitani *et al* proposed that nickel atoms occupy only the Cu(2) site according to their x-ray and neutron diffraction results [41], while Bridges *et al* [42] performed XAFS experiments and concluded that nickel substitutes nearly uniformly on both Cu sites. For zinc, Kajitani *et al* showed that a ratio between occupancies of the Cu(1) and Cu(2) sites was 4 : 1 (the ratio between the zinc amounts on both sites was 2 : 1 because the Cu site ratio is 1 : 2). Roth *et al* [43] reported another value of 2 : 1 for the occupancy ratio. On the contrary to these results, Maeda *et al* [44] and Yang *et al* [45] claimed from their EXAFS experiments that zinc substitutes only on the Cu(2) site. In the present work, considering the above mentioned situation, we performed calculations on models (*a*)–(*c*) for iron and on the models (*c*) and (*d*) for nickel or zinc.

Examples of calculated positron distributions are shown in figure 4. Panels (*a*)–(*e*) correspond to the results for iron on model (*c*), nickel on models (*c*) and (*d*), and zinc on models (*c*) and (*d*), respectively. It can be seen that iron, nickel and zinc atoms tend to repulse positrons and iron shows a much larger effect compared with the others. The calculated lifetimes and energy eigenvalues of positrons are listed in table 2 together with those for the non-doped YBCO. The values in brackets correspond to the difference of the energy eigenvalues for the doped and non-doped YBCO. The predicted variation of lifetimes is quite small and at most 3 ps. On the contrary, remarkable increases of the energy eigenvalues are observed for iron substitution as well as nickel on the Cu(1) site.

3. Sample preparation and characterization

The samples of $YBa_2(Cu_{1-x}M_x)_3O_{7-y}$ (M = Fe, Ni, Zn) were prepared by a conventional solid state reaction method. Starting materials were high-purity powders of Y_2O_3, $BaCO_3$, CuO and Fe_2O_3/NiO/ZnO. These powders were thoroughly mixed in their nominal compositions. The resultant mixture was firstly reacted at 890–910 °C for 10–25 hours. The products were calcined at 890–940 °C for 10–50 hours and this calcination procedure was repeated with pulverization between the steps until no second phase had been observed in the x-ray diffraction pattern. The final products were pulverized again and pressed into pellets with diameter 8.8 mm and thickness 1.5 mm. These pellets were sintered at 930 °C for 20 hours followed by annealing at 400 °C for 10 hours. All of these heat treatments were performed in O_2 flow. The cooling from 930 °C to 400 °C was done slowly at a rate of 0.5 °C min^{-1}.

The samples prepared were characterized by x-ray diffraction and by resistivity measurements using a conventional DC four-probe method. The variations of the lattice parameters with impurity doping are shown in figure 5. An apparent structural change from orthorhombic to tetragonal is observed for the iron substituted samples with increasing iron content, while neither the nickel nor zinc substitution causes such a structural transition. These features are in good agreement with previous studies [46]. The resistivity–temperature curves for non-doped, iron-doped, nickel-doped and zinc-doped samples are shown in figure 6(*a*)–(*d*), respectively. In figure 7, T_c (midpoint) is presented as a function of impurity concentration. The observed T_c decreases monotonically with increasing x for the nickel or zinc-doped specimen, while, for the iron-doped one, there is a plateau in a low-x region. Such behaviour has also been observed in other studies [45, 46].

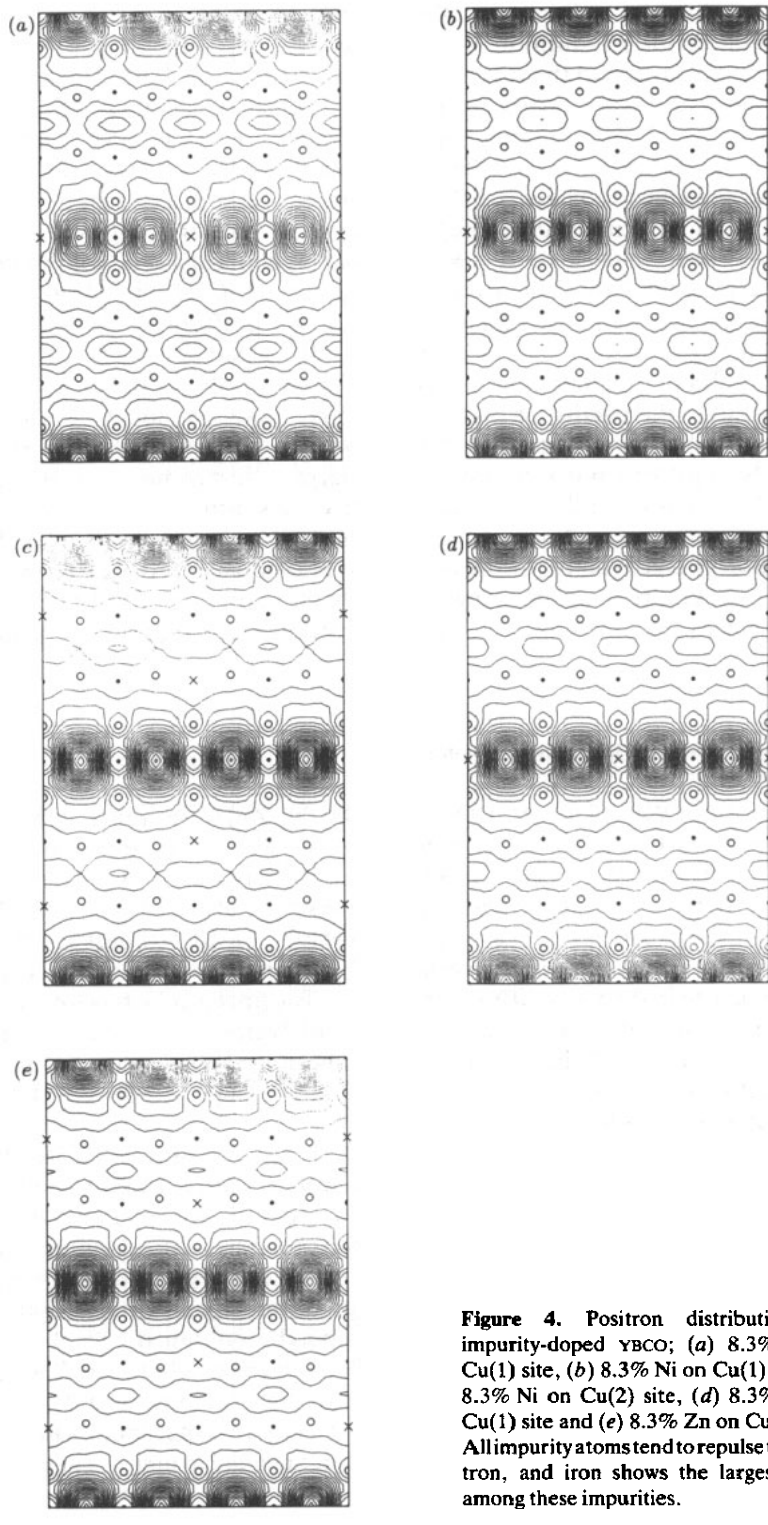

Figure 4. Positron distributions in impurity-doped YBCO; (*a*) 8.3% Fe on Cu(1) site, (*b*) 8.3% Ni on Cu(1) site, (*c*) 8.3% Ni on Cu(2) site, (*d*) 8.3% Zn on Cu(1) site and (*e*) 8.3% Zn on Cu(2) site. All impurity atoms tend to repulse the positron, and iron shows the largest effect among these impurities.

Table 2. The calculated positron lifetime and energy eigenvalue for doped YBCO. Values shown in brackets are the differences from the eigenvalue of non-doped YBCO. The variation of lifetime is quite small (<3 ps), while the energy eigenvalue shows a distinct increase with substitution, especially for the iron case.

Dopant	Positron lifetime	Energy eigenvalue
None	159 ps	1.680 eV (—)
Fe 2.1% on Cu(1)	158 ps	1.704 eV (24 meV)
Fe 4.2% on Cu(1)	158 ps	1.731 eV (51 meV)
Fe 8.3% on Cu(1)	156 ps	1.790 eV (110 meV)
Ni 8.3% on Cu(1)	157 ps	1.745 eV (65 meV)
Ni 8.3% on Cu(2)	160 ps	1.691 eV (11 meV)
Zn 8.3% on Cu(1)	158 ps	1.704 eV (24 meV)
Zn 8.3% on Cu(2)	159 ps	1.684 eV (4 meV)

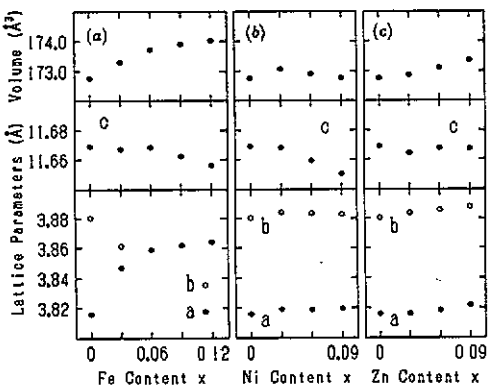

Figure 5. Variations of lattice parameters with impurity doping; (*a*) Fe, (*b*) Ni and (*c*) Zn. For iron doping, the transition from an orthorhombic structure to a tetragonal one occurs around $x = 0.03$. No transition was observed for nickel and zinc substitutions.

4. Positron lifetime measurements

The positron lifetime spectra were measured using a fast–fast lifetime spectrometer with a resolution of 190–220 ps full-width at half-maximum (FWHM). The positron source was prepared by depositing a ^{22}NaCl solution on a 7.5 μm thick Kapton sheet and covering it with another Kapton sheet. The measuring temperature was controlled between 20 K and room temperature using a helium cryogenic apparatus in a vacuum chamber with a heater, and it was monitored with a Au(0.07 at.% Fe)/Chromel thermocouple. About 10^6 counts were accumulated for each spectrum.

The obtained spectra were analysed using the PATFIT program [47] and divided into two components besides a source component. The short conponent, which is denoted in the following as τ_1, is considered to be the positron lifetime in the bulk state which is modified due to the existence of positron trapping into defects. The long one, denoted as τ_2, is the lifetime in the defects. The intensities of these components are denoted as I_1 and I_2. The mean lifetime τ_{mean} is obtained as $\tau_{mean} = \tau_1 I_1 + \tau_2 I_2$. The bulk lifetime τ_{bulk} was calculated, assuming the validity of the simple two state trapping model, as $\tau_{bulk} = [I_1/\tau_1 + I_2/\tau_2]^{-1}$. The resultant temperature dependences of the positron lifetime parameters such as τ_2, τ_{mean}, τ_{bulk} and I_2 for non-doped, iron-doped, nickel-doped or

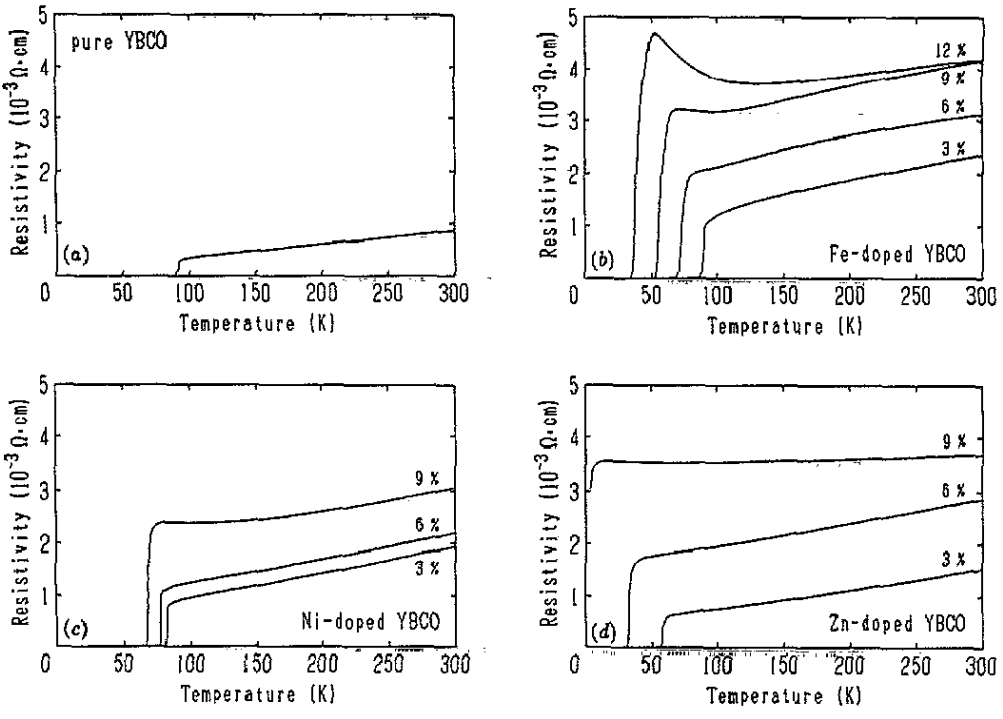

Figure 6. Resistivity–temperature curves for (*a*) non-doped, (*b*) Fe-doped, (*c*) Ni-doped and (*d*) Zn-doped specimens. Resistivity increases with each increasing dopant content while the temperature coefficient decreases.

zinc-doped YBCO are shown in figures 8–11, respectively. We have summarized the important features in the following.

4.1. Non-doped YBCO

The mean lifetime τ_{mean} shows an increase from 193 ps to 203 ps in the temperature region of 20–100 K, and keeps nearly constant between 100–180 K and then decreases by approximately 20 ps as the temperature increases to room temperature. Such behaviour was also observed in the temperature dependence of the S parameter [14, 16, 18, 19]. The defect-related component τ_2 shows a step-like increase from 215 ps to 230 ps and this transition region is ranged between 50 and 100 K. This change reflects the thermal variation of τ_{mean}. The bulk lifetime is almost a constant value of 175–180 ps below 100 K, while, above that, it shows a slow decrease. It can be seen that the former belongs to the first-type category mentioned in section 1 while the latter belongs to the second-type.

4.2. Iron-doped YBCO

Systematic variations of the thermal behaviour of τ_{mean} with iron substitution are observed as in the preliminary work [28, 29]. The temperature range in which τ_{mean} increases is expanded and shifted towards a higher temperature. This corresponds to

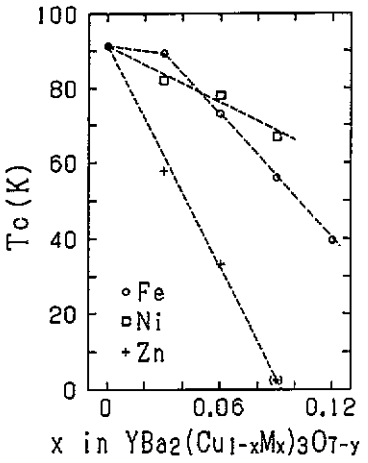

Figure 7. T_c (mid point) variation with dopant concentration. T_c decreases monotonically with nickel and zinc doping, while, for iron doping, the T_c variation is small in the range of $x < 0.03$. Zinc shows a remarkable T_c suppressing effect.

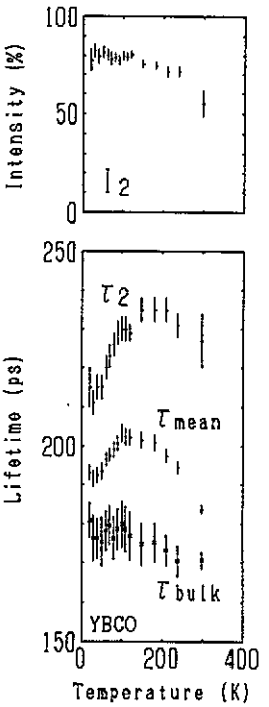

Figure 8. Temperature variation of positron lifetime parameters in non-doped YBCO. Either τ_2 or τ_{mean} show a step-like increase between 50 and 100 K, while τ_{bulk} has a slight decrease above 100 K.

the variation of τ_2. The decrease of τ_{mean} above 180 K is removed with the iron doping. The bulk lifetime is also affected by the substitution but less dramatically. Its temperature variation curve becomes structureless with the substitution.

4.3. Nickel-doped YBCO

The thermal behaviour of τ_{mean} is altered little by the substitution. The convergence of τ_2 (as well as τ_1) is not so good, probably reflected by the existence of various configurations of defect–impurity. Values of τ_2 at room temperature are not shown in the figure. The values are in the range 270–300 ps and show a discontinuous leap at 240 K. However, this is considered to be an artefact in the fitting procedure due to the small value of its intensity I_2. Such a leap was also observed in the 3% or 6% zinc-doped specimen. The nickel substitution effect on the temperature–τ_2 curve is ambiguous, which is different from the results for the iron-doped YBCO. On the other hand, τ_{bulk} shows a very distinct substitution dependence. With doping of $x = 0.03$, the τ_{bulk} decreasing region is extended to a lower temperature compared with the undoped specimen. The temperature variation curve is nearly structureless at $x = 0.06$. At $x = 0.09$, the increase in the low-temperature region (<80 K) becomes distinct.

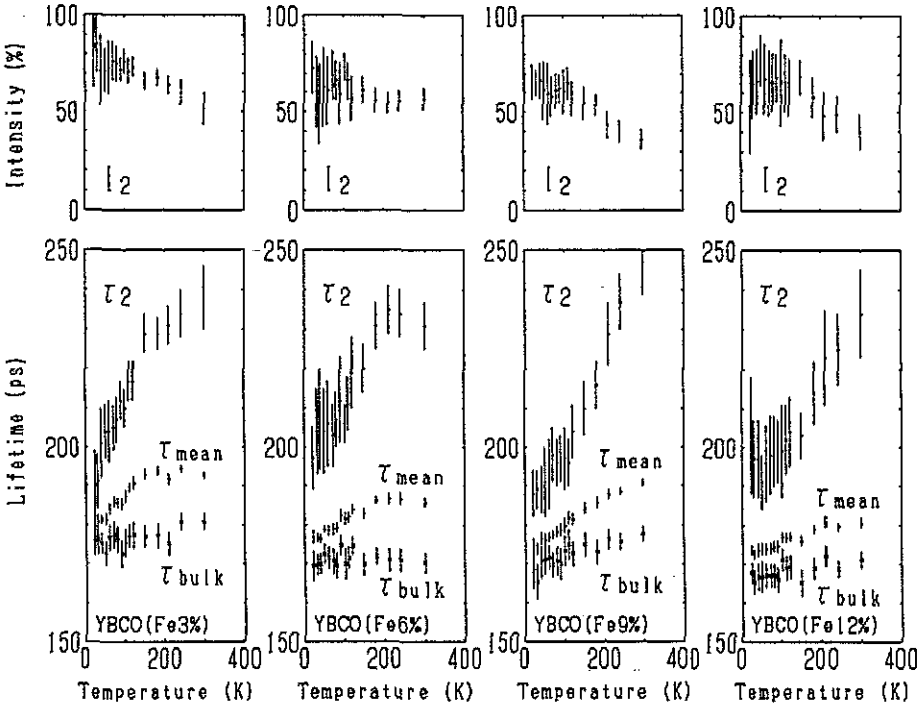

Figure 9. Temperature variation of positron lifetime parameters in Fe-doped YBCO.

4.4. Zinc-doped YBCO

The temperature variation curve of each parameter shows a similar x-dependence as for the nickel-doped specimens although zinc is quite different from nickel in the T_c suppression effect. One distinction is the noticeable variation of the absolute value of τ_{bulk} with x at higher temperatures.

5. Discussion

As for the positron distribution in the perfect crystal of pure YBCO, the present results are in rather good agreement with other results reported by several groups [16, 48–52]. The calculated positron lifetime of 159 ps is the same value obtained by Jensen *et al* [48] while the experimental value at room temperature is ~170 ps in the present work. The discrepancy between the experimental and calculated values is thought to be mostly due to the oxygen deficiency.

The distribution of positrons trapped at an isolated oxygen vacancy is extended over a region of $5a_0 \times 5b_0$ (a_0, b_0: lattice parameters) in the ab plane. If all oxygen vacancies are isolated, non-stoichiometry ranged between 0.05–0.10 means that there is one vacancy per area of $3a_0 \times 3b_0$–$4.5a_0 \times 4.5b_0$. In this case, a positron state centred on a vacancy overlaps and there is no longer a localized state. Then, in the real material, with oxygen deficiency $y = 0.05$–0.10, the positron lifetime in the bulk is expected to be close to 170 ps corresponding to the isolated oxygen vacancy. If aggregation of oxygen

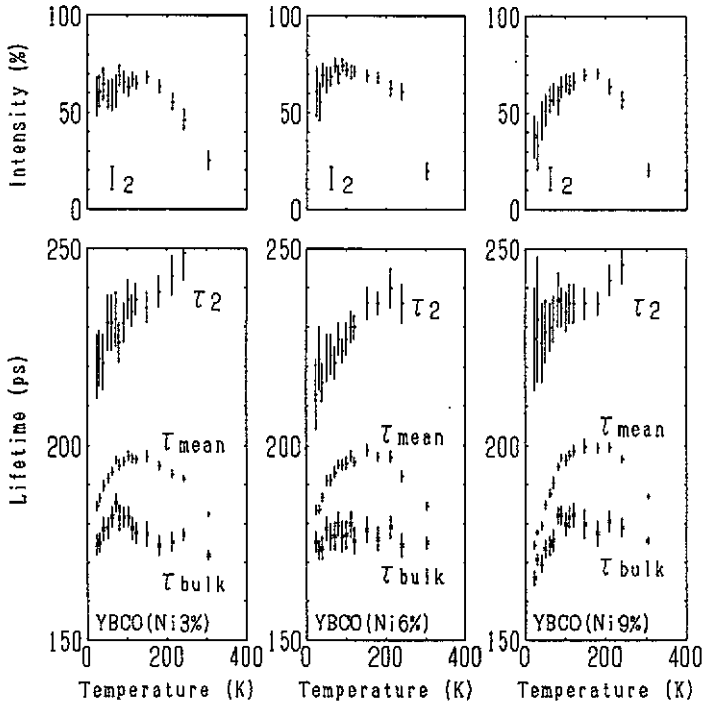

Figure 10. Temperature variation of positron lifetime parameters in Ni-doped YBCO.

vacancies occurs, the volume in which one cluster of oxygen vacancies is expected to exist will expand while the positron distribution itself will be confined. A localized state remains for such a case. The thermal energy corresponding to room temperature is 25 meV. Since the estimated positron binding energies to the oxygen vacancy clusters are 70–270 meV and are not so large compared with the thermal energy, thermally activated positron detrapping should occur in the experimental temperature range between 20 K and room temperature.

As for other defects, e.g. cation vacancies, Jensen *et al* performed similar calculations and predicted lifetime values of more than 200 ps [48].

Impurity substitution effects were also examined by Jean *et al* [51] and Bharathi *et al* [52]. Both concluded that zinc substitution causes a change of positron distribution from an almost localized state between Cu–O one-dimensional chains to a rather uniform one. Their conclusion is in contrast with our result which shows little change of positron distribution with zinc substitution. In part, the discrepancy seems to be owing to an extremely high substitution concentration assumed in their calculations.

If we assume two types of positron trapping centres (shallow and deep traps), the step-like increase of τ_2 can be interpreted as follows. τ_2 is a weighted average of positron lifetimes at both defects. At low temperature, each defect traps a positron with a probability which is determined by the concentration and a specific positron trapping rate of the defect. When the temperature increases, thermal detrapping from the shallow traps occurs above a certain temperature and the contribution to the total event from annihilations at the shallow traps begins to decrease. Generally speaking, the lifetime

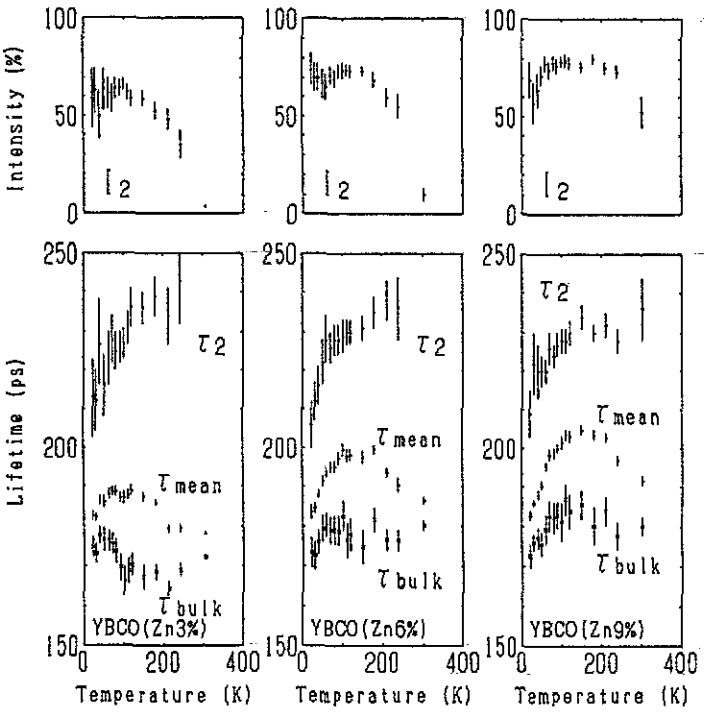

Figure 11. Temperature variation of positron lifetime parameters in Zn-doped YBCO.

of a positron trapped in a shallow trap is shorter than that in a deeper trap. Then, τ_2 would show a step-like increase.

Another possible interpretation for the step-like increase of τ_2 employs only one type of defect. In this case, the transition of τ_2 is ascribed to a variation of the defect's charge state. Corbel *et al* claimed that detrapping of a positron from the defect, corresponding to the lifetime of about 225 ps, is unlikely because a higher binding energy is expected for such a long lifetime and they supported this one-defect model [21]. However, it should be noted that, in the two-defect model, τ_2 is an average value of the two lifetimes and we can assume one is nearly equal to the bulk lifetime. From this point of view, the detrapping is likely.

The present results of iron substitution support the two-defect model. The theoretical calculation predicts that iron substitution enhances the energy eigenvalue of a positron in the bulk state. Since the energy of a positron trapped at a defect is determined only by the local environment, we can use the value of a non-doped material in a dilute region. The binding energy between the positron and the defect is expected to increase with iron substitution. The experimentally observed shift of the transition region of τ_2 can be explained by this effect.

Another iron substitution effect is the elimination of the decrease of τ_{mean} in the range 180–300 K. This decrease can be attributed to the positron detrapping from the deeper trap [19]. Because of the same reason as in the case of shallow trap, the binding energy between the positron and the deeper trap is enhanced with iron substitution. For this reason, the region in which τ_{mean} decreases is shifted out of the measured temperature range.

In contrast with the iron case, such shifts were not observed for nickel or zinc substitution. This is quite reasonable for zinc because the estimated differences of the positron energy are small. As for nickel, the estimated difference for substitution on the Cu(1) site is considerable. Then, a large part of nickel should be occupying the Cu(2) site.

Finally, we discuss the temperature variation of τ_{bulk}. A positron lifetime in the superconducting state has been treated theoretically by several authors. Previously, Dresden proposed enhancement of the positron lifetime in the superconducting state of metals [53], but subsequent experiments did not find any variations of the positron lifetime [54, 55]. Tripathy and Bhuyan also estimated positron lifetime in aluminium and concluded that the lifetime in the superconducting state should be 10^4 times longer than that in the normal state [56]. No experimental confirmation, however, has been obtained. After the discovery of the oxide superconductor, several theoretical models have been proposed to explain the distinct variation of positron lifetimes. McMullen performed an estimation in terms of BCS theory and claimed that the observed lifetime variation cannot be explained by a model based on BCS theory [57]. He also tried another calculation based on the RVB model [58]. Although this model can reproduce the lifetime–temperature curves obtained on YBCO single-crystal [24] as well as other oxides [59, 60], some difficulties still remain. Chakraborty noted that annihilations occur predominantly with tight-binding core-like electrons and introduced a model in which heavy holes are assumed to distribute on the two-dimensional lattice [61]. He expected that the overlap of a positron and the tight-binding electrons will be altered by hole condensations accompanying the superconducting transition. The above-mentioned models focus on the correlation between a positron and electrons. Jean *et al* [51] as well as Bharathi *et al* [52] proposed a so-called charge–transfer model. They claimed that the temperature dependence of positron annihilation parameters below T_c can be understood in terms of an electron density transfer from the planar oxygen atoms to the apical oxygen atoms.

τ_{bulk} measured in the present work shows a temperature variation not only in the superconducting state but also in the normal state. In pure YBCO, τ_{bulk} is nearly constant in the superconducting state, while in the normal state it shows a smooth decrease. On the other hand, τ_{bulk} shows a distinct increase between 20 and 70 K in 9% zinc-doped YBCO, although the specimen is not superconducting in the measurement temperature range of 20–300 K.

In pure YBCO, as well as in low nickel or zinc content specimens, each curve seems to have a shoulder or a hump near T_c. On the other hand, there is no definite structure for iron doped samples and, in 9% zinc-doped samples, the τ_{bulk}–temperature curve shows a shoulder at a much higher temperature than T_c.

It seems to be impossible to explain the variation of τ_{bulk} in the normal state in terms of the pairing itself. The models based on the BCS theory [56, 57] or hole pairing [61] are not able to be applied to interpreting the current results, especially the result for a 9% zinc-doped specimen. Although the only model to explain the variation in the normal state is McMullen's model, which is based on the RVB theory [57], it still contains some difficulties—as mentioned above. Besides the correlation to the superconductivity itself, there are some possible origins for the variations of τ_{bulk}: (1) an electron density variation resulting from structural change, charge transfer or redistribution of positrons, (2) variation of the positron–electron correlation, and (3) a large anharmonic oscillation of the O (1) ion on a one-dimensional chain [16]. Quantitative treatments have not yet been accomplished.

Jean *et al* also examined the substitution effect on τ_{bulk} in the case of zinc and gallium [51]. They reported a τ_{bulk} variation with substitution at room temperature from ~190 ps

for the pure sample to ~130 ps for the 7% zinc-doped sample or ~210 ps for the 7% gallium-doped sample. Such a variation seems to be too drastic, however.

As for the temperature variation of τ_{bulk} in YBCO, there are, so far, a few experimental reports [24, 29, 51], which differ from each other. Theoretical explanations still remain in a semi-quantitative regime.

6. Conclusion

We have carried out measurements of the temperature variation of positron lifetime parameters in $YBa_2(Cu_{1-x}M_x)_3O_{7-y}$ (M = Fe, Co, Ni). The defect related component τ_2 shows a step-like increase in the temperature range of 60–100 K on the pure sample. When accompanied with iron substitution, this transition region was shifted to a higher temperature. On the other hand, no such shift was observed in the nickel or zinc substitution case. These phenomena can be plausibly interpreted in terms of a thermal escape of a positron from a shallow trapping centre and a variation of the positron–defect binding energy with impurity substitution. We have also observed systematic changes of the temperature variation curves of τ_{bulk}. Further work is needed to reveal the origin of these changes.

Acknowledgments

The authors are grateful to Drs A Matsushita and Y Yamada for their assistance in the preparation and characterization of the samples, and to Mr T Kaneko and A Yamaguchi for their kind cooperation in the experiments. This work was partially supported by the Grant-in-Aid for Scientific Research on Chemistry of New Superconductors.

References

[1] Bednorz J G and Müller K A 1986 *Z. Phys.* B **64** 189
[2] Kishio K, Kitazawa K, Kanbe S, Yasuda I, Sugii N, Takagi H, Uchida S, Fueki K and Tanaka S 1987 *Chem. Lett.* 429
[3] Wu M K, Ashburn J R, Torng C J, Hor P H, Gao R L, Huang Z, Wang Y Q and Chu C W 1987 *Phys. Rev. Lett.* **58** 908
[4] Maeda H, Tanaka Y, Fukutomi M and Asano T 1988 *Japan. J. Appl. Phys.* **27** L209
[5] Sheng Z Z and Herman A M 1988 *Nature* **322** 55
[6] See, for example,
Brandt W and Dupasquier A (ed) 1983 *Positron Solid State Physics* (Amsterdam: North-Holland)
[7] See, for example,
Haghighi H, Kaiser J H, Rayner S, West R N, Fluss M J, Howell R H, Turchi P E A, Wachs A L, Jean Y C and Wang Z Z 1990 *J. Phys.: Condens. Matter* **2** 1911 and references therein
[8] Ishibashi S, Yamaguchi A, Suzuki Y, Doyama M, Kumakura H and Togano K 1987 *Japan. J. Appl. Phys.* **26** L688
[9] Manuel A A 1989 *J. Phys.: Condens. Matter* **1** SA107
[10] Jean Y C, Wang S J, Nakanishi H, Hardy W N, Hayden M E, Kiefl R F, Meng R L, Hor H P, Huang J Z and Chu C W 1987 *Phys. Rev.* B **36** 3994
[11] Usmar S G, Sferlazzo P, Lynn K G and Moodenbaugh A R 1987 *Phys. Rev.* B **36** 8854
[12] Smedskjaer L C, Veal B W, Legnini D G, Paulikas A P and Nowicki L J 1988 *Phys. Rev.* B **37** 2330
[13] Doyama M, Yamamoto R, Suzuki Y, Ishibashi S, Yamaguchi A, Kumakura H and Togano K 1987 *Physica* **148B** 497
[14] Lynn K G, Usmar S G, Nielsen B, van der Kolk G J, Kanazawa I, Sferlazzo P and Moodenbaugh A R 1988 Thin film processing and characterization of high-temperature superconductors *AIP Conf. Proc.*

No 165 (*American Vacuum Society Series No 3*) ed J M E Harper, R J Cotton and L C Feldman (New York: American Institute of Physics) p 435
[15] Charalambous S, Chardalas M, Dedoussis S, Elefteriades C, Liolios A K and Niarchos D 1988 *Phys. Lett.* A **128** 97
[16] von Stetten E C, Berko S, Li X S, Lee R R, Brynestad J, Singh D, Krakauer H, Pickett W E and Cohen R E 1988 *Phys. Rev. Lett.* **60** 2198
[17] Sundar C S, Sood A K, Bharathi A and Hariharan Y 1988 *Physica* C **153–155** 155
[18] Usmar S G, Lynn K G, Moodenbaugh A R, Suenaga M and Sabatini R L 1988 *Phys. Rev.* B **38** 5126
[19] Brusa R S, Grisenti R, Liu S, Oss S, Pilla O, Zecca A, Dupasquier A and Matacotta F A 1988 *Physica* C **156** 65
[20] Matsui M, Numata H, Matsuoka H, Shimizu T, Doyama M, Ishibashi S, Suzuki Y, Yamamoto R 1989 *Positron Annihilation* ed L Dorikens-Vanpraet, M Dorikens and D Segers (Singapore: World Scientific) p 928
[21] Corbel C, Bernede P, Pascard H, Rullier-Albenque F, Korman R and Marucco J F 1989 *Appl. Phys.* A **48** 335
[22] Ishibashi S, Suzuki Y, Yamamoto R, Hatano T, Ogawa K and Doyama M 1988 *Phys. Lett.* A **128** 387
[23] Ishibashi S, Suzuki Y, Maruyama H, Yamamoto R and Doyama M 1989 *Positron Annihilation* ed L Dorikens-Vanpraet, M Dorikens and D Segers (Singapore: World Scientific) p 925
[24] Harshman D R, Schneemeyer L F, Waszczak J V, Jean Y C, Fluss M J, Howell R H and Wachs A L 1988 *Phys. Rev.* B **38** 848
[25] Teng M K, Shen D X, Chen L, Yi C Y and Wang G H 1987 *Phys. Lett.* A **124** 363
[26] Zhu J S, Song J X, Wang J, Yang Z J, Zhang Y and Lung C W 1988 *J. Phys. C: Solid State Phys.* **21** L281
[27] Krištiaková K, Šauša O, Krištiak J and Jánoš Š 1989 *Z. Phys.* B **71** 197
[28] Ishibashi S, Suenaga K, Yamamoto R, Doyama M and Matsumoto T 1990 *J. Phys.: Condens. Matter* **2** 3691
[29] Ishibashi S, Yamamoto R, Doyama M and Matsumoto T 1990 *J. Less-Common Met.* **164–165** 1113
[30] Puska M J and Nieminen R M 1983 *J. Phys. F: Met. Phys.* **13** 333
[31] Boroński E and Nieminen R M 1986 *Phys. Rev.* B **34** 3820
[32] Herman F and Skillman S 1963 *Atomic Structure Calculations* (New Jersey: Prentice-Hall)
[33] Kimball G E and Shortley G H 1934 *Phys. Rev.* **45** 815
[34] Brandt W and Reinheimer J 1971 *Phys. Lett.* A **35** 109
[35] Jorgensen J D, Veal B W, Paulikas A P, Nowicki L J, Crabtree G W, Claus H and Kwok W K 1990 *Phys. Rev.* B **41** 1863
[36] Xu Y, Suenaga M, Tafto J, Sabatini R L, Moodenbaugh A R and Zolliker P 1989 *Phys. Rev.* B **39** 6667
[37] Roth G, Heger G, Renker B, Pannetier J, Caignaert V, Hervieu M and Raveau B 1988 *Z. Phys.* B **71** 43
[38] Bordet P, Hodeau J L, Strobel P, Marezio M and Santoro A 1988 *Solid State Commun.* **66** 435
[39] Katano S, Matsumoto T, Matsushita A, Hatano T and Funahashi S 1990 *Phys. Rev.* B **41** 2009
[40] Yang C Y, Heald S M, Tranquada J M, Xu Y, Wang Y L and Moodenbaugh A R 1989 *Phys. Rev.* B **39** 6681
[41] Kajitani T, Kusaba K, Kikuchi M, Syono Y and Hirabayashi M 1988 *Japan. J. Appl. Phys.* **27** L354
[42] Bridges F, Boyce J B, Claeson T, Geballe T H and Tarascon J M 1990 *Phys. Rev.* B **42** 2137
[43] Roth G, Adelmann P, Ahrens R, Blank B, Bürkle H, Gompf F, Heger G, Hervieu M, Nindel M, Obst B, Pannetier J, Raveau B, Renker B, Rietschel H, Rudolf B and Wühl H 1989 *Physica* C **162–164** 518
[44] Maeda H, Koizumi A, Bamba N, Takayama-Muromachi E, Izumi F, Asano H, Shimizu K, Moriwaki H, Maruyama H, Kuroda Y and Yamazaki H 1989 *Physica* C **157** 483
[45] Yang C Y, Moodenbaugh A R, Wang Y L, Xu Y, Heald S M, Welch D O, Suenaga M, Fischer D A and Penner-Hahn J E 1990 *Phys. Rev.* B **42** 2231
[46] See, for example, Tarascon J M, Barboux P, Miceli P F, Greene L H, Hull G W, Eibschutz M and Sunshine S A 1988 *Phys. Rev.* B **37** 7458
[47] Kirkegaard P, Eldrup M, Mogensen O E and Pedersen N J 1981 *Comput. Phys. Commun.* **23** 307
[48] Jensen K O, Nieminen R M and Puska M J 1989 *J. Phys.: Condens. Matter* **1** 3727
[49] Bharathi A, Sundar C S and Hariharan Y 1989 *J. Phys.: Condens. Matter* **1** 1467
[50] Singh D, Pickett W E, Cohen R E, Krakauer H and Berko S 1989 *Phys. Rev.* B **39** 9667
[51] Jean Y C, Sundar C S, Bharathi A, Kyle J, Nakanishi H, Tseng P K, Hor P H, Meng R L, Huang Z J, Chu C W, Wang Z Z, Turchi P E A, Howell R H, Wachs A L and Fluss M J 1990 *Phys. Rev. Lett.* **64** 1593
[52] Bharathi A, Sundar C S, Ching W Y, Jean Y C, Hor P H, Xue Y Y and Chu C W 1990 *Phys. Rev.* B **42** 10199

[53] Dresden M 1954 *Phys. Rev.* **93** 1413
[54] Green B and Madansky L 1956 *Phys. Rev.* **102** 1014
[55] Shafroth S M and Marcus J A 1956 *Phys. Rev.* **103** 585
[56] Tripathy D N and Bhuyan M 1985 *Positron Annihilation* ed P C Jain, R M Singru and K P Gopinathan (Singapore: World Scientific) p 91
[57] McMullen T 1990 *Phys. Rev.* B **41** 877
[58] Rice M J and Wang Y R 1988 *Phys. Rev.* B **37** 5893
[59] Jean Y C, Kyle J, Nakanishi H, Turchi P E A, Howell R H, Wachs A L, Fluss M J, Meng R L, Hor H P, Huang J Z and Chu C W 1988 *Phys. Rev. Lett.* **60** 1069
[60] Jean Y C, Nakanishi H, Fluss M J, Wachs A L, Turchi P E A, Howell R H, Wang Z Z, Meng R L, Hor P H, Huang Z J and Chu C W 1989 *J. Phys.: Condens. Matter* **1** 2989
[61] Chakraborty B 1989 *Phys. Rev.* B **39** 215